GEOCHEMISTRY

Potassium isotopic heterogeneity in subducting oceanic plates

Yan Hu[1]*, Fang-Zhen Teng[1]*, Terry Plank[2], Catherine Chauvel[3,4]

Oceanic crust and sediments are the primary K sinks for seawater, and they deliver considerable amounts of K to the mantle via subduction. Historically, these crustal components were not studied for K isotopes because of the lack of analytical precision to differentiate terrestrial variations. Here, we report a high-precision dataset that reveals substantial variability in oceanic plates and provides further insights into the oceanic K cycle. Sixty-nine sediments worldwide yield a broad δ^{41}K range from −1.3 to −0.02‰. The unusually low values are indicative of release of heavy K during continental weathering and uptake of light K during submarine diagenetic alteration. Twenty samples of altered western Pacific crust from ODP Site 801 display δ^{41}K from −0.60 to −0.05‰, averaging at −0.32‰. Our results indicate that submarine alteration of oceanic plates is essential for generating the high-δ^{41}K signature of seawater. These regionally varying subducting components are heterogeneous K inputs to the mantle.

INTRODUCTION

Oceanic crust and seafloor sediments play an essential role in modifying the chemical and isotopic composition of seawater; they are also a primary input of volatile compounds and crust-enriched elements to subduction zones that leads to mantle heterogeneity (*1*–*3*). Elevated potassium (K) contents in basalts have been used as an indicator of such heterogeneity (*4*) because K concentration is substantially higher in oceanic crust [~1000 parts per million (ppm) (*5*, *6*)] and marine sediments [18,350 ppm (*2*)] relative to the mantle [260 ppm (*7*)]. The basaltic crust further accumulates K (~5000 ppm) during low-temperature hydrothermal circulation (*8*–*10*). Therefore, altered crust is an important K sink for seawater, along with authigenic mineral formation in marine sediments (*9*–*16*). Potassium has two stable isotopes with mass 39 (93.3%) and 41 (6.7%), and variation in the K isotopic ratio provides a rare opportunity to constrain mass fluxes of crustal recycling from a major element perspective. However, because of previous limitations in analytical precision, terrestrial variations were unresolvable within ±0.5‰ (*17*). This study leverages recently developed methods to provide high-precision [better than 0.06‰ (*18*)] measurements and further insights into K isotopic variations in altered oceanic crust and subducting sediments, the two major components of crustal cycling.

Markedly improved analytical precision of δ^{41}K [$\delta^{41}K\ (‰) = ((^{41}K/^{39}K)_{sample}/(^{41}K/^{39}K)_{standard} - 1) \times 1000$] allows identification of K-rich crustal materials that are recycled to the mantle. Studies of an Iceland's basalt-to-rhyolite differentiation sequence suggest negligible K isotope fractionation (<0.1‰) during mantle partial melting and magmatic differentiation (*19*), which is supported by theoretically calculated fractionations between silicate melts and minerals at equilibrium (*20*). Hence, δ^{41}K values in basalts are representative of their mantle sources. Fresh oceanic basalts sampled globally have δ^{41}K values that range from −0.66 to −0.25‰, with 90% of the samples clustering between −0.52 and −0.34‰ (fig. S1), indicating a relatively homogeneous K isotopic composition of the global ambient mantle (*19*, *21*). A suite of continental basalts from northeastern China displays a noticeably larger variation (−0.81 to −0.15‰), and their δ^{41}K values correlate with elemental ratios and radiogenic isotopes that are indicative of crustal inputs (*22*). These correlations suggest modification of their mantle sources by recycled crustal components (*22*). While large K isotopic variations have been documented in sedimentary materials on continents (*23*–*26*), the K isotopic compositions of crustal materials that are presently entering the subduction zones are poorly constrained. These components are the focus of the current study.

Marine sediments and underlying basaltic crust are two primary K sinks for the ocean. Constraining their K isotopic variations is critical for identifying their roles in the oceanic K cycle. The oceanic K cycle is largely controlled by continental silicate weathering and marine authigenic aluminosilicate formation; both processes are linked to the long-term carbon cycle (*15*). A major discovery from recent high-precision K isotope studies is that seawater is isotopically 0.55‰ heavier than average igneous rocks (*27*–*29*). With a homogeneous δ^{41}K value of 0.12 ± 0.07‰, seawater constitutes the isotopically heaviest K reservoir on Earth (*30*, *31*). This high δ^{41}K value cannot be accounted for by K inputs from dissolved riverine loads or mid-ocean ridge hydrothermal fluids, both of which are isotopically lighter than seawater (*25*, *32*). Therefore, there must be oceanic sinks that remove light K isotopes from seawater. The major K sinks include low-temperature alteration of basaltic crust and authigenic mineral formation in marine sediments. Depth profiles of δ^{41}K in sediment pore fluids suggest removal of isotopically light K (*33*), yet this removal cannot be unambiguously attributed to marine sediments or the underlying oceanic crust (*15*). On the other hand, two recent studies on altered basalts, including samples from ophiolite suites and ocean drilling cores, reached inconsistent conclusions regarding the magnitude and direction of K isotope fractionation during low-temperature hydrothermal alteration (*34*, *35*). These disparate findings motivated us to further investigate the behavior of K isotopes during submarine alteration of oceanic crust and sediments and how these alteration processes affect the oceanic δ^{41}K signature.

The samples analyzed here include marine cores of altered basaltic crust and sediments drilled in front of major subduction zones around the globe (fig. S2). The basaltic basement core was recovered from Ocean Drilling Program (ODP) Site 801, which lies seaward of the Mariana Trench and represents the majority of the subducting western Pacific crust. As the oldest drilled oceanic basement [ca. 170 million

[1]Isotope Laboratory, Department of Earth and Space Sciences, University of Washington, Seattle, WA 98195, USA. [2]Lamont-Doherty Earth Observatory, Columbia University, Palisades, NY 10964-8000, USA. [3]Université de Paris, Institut de Physique du Globe de Paris, CNRS, F-75005 Paris, France. [4]Université Grenoble Alpes, ISTerre, CNRS, F-38041 Grenoble, France.
*Corresponding author. Email: yanhu@uw.edu (Y.H.); fteng@uw.edu (F.-Z.T.)

years (Ma) (*36*)], it preserves a long history of low-temperature alteration and is a reference section for altered basement formed at fast-spreading ridges (*10*, *37*, *38*). The sediment cores encompass a wide variety of sedimentary materials that were used to constrain the bulk composition of global subducting sediments (*2*). Overall, our study provides direct evidence that low-temperature alteration of oceanic crust and authigenic mineral formation during sediment diagenesis preferentially remove light K isotopes from seawater, thereby leading to its heavy K isotopic composition. These fractionation processes impart distinct $\delta^{41}K$ signatures in altered basaltic crust and sediments that can be used to identify their contributions to the mantle.

RESULTS

The $\delta^{41}K$ values measured in altered crust vary from −0.60 to −0.05‰ and in subducting sediments from −1.3 to −0.02‰ (tables S1 and S2); these values span a range of 20 times greater than the long-term precision of our analytical methods. The $\delta^{41}K$ data straddle the average mantle value of −0.43‰ (*21*); however, they are all lower than the seawater value of 0.12‰ (see Materials and Methods for sample details) (*30*, *31*).

Altered basaltic crust from western Pacific

The upper oceanic basement at ODP Site 801 formed in two stages: The 315-m lower unit represents the Pacific crust formed at the spreading ridges around 167.4 Ma (on-axis), and the 175-m upper unit represents off-axis sill intrusions into the basal sediments at around 160.1 Ma (*36*). Both units are altered by low-temperature hydrothermal fluids (*10*). The basement core analyzed here includes individual samples and composite mixtures made by reconstituting the various lithologies in proportions to their abundance at a given depth (*8*). Compared with fresh basaltic glass from the core, altered basalts are enriched in K_2O to various extents (Fig. 1A). There is a concomitant increase in K_2O and $\delta^{41}K$ upward in the core (Fig. 1). Eight individual samples that encompass a broad range of alteration have $\delta^{41}K$ values between −0.60 and −0.29‰. A single sample from the hydrothermal layer at 625 mbsf (meters below the seafloor) was also analyzed. It is composed mainly of iron oxyhydroxides cemented by quartz (*10*), and it has an exceptionally high $\delta^{41}K$ value of −0.05‰. Ten composite samples have $\delta^{41}K$ values ranging from −0.49 to −0.31‰, and samples from the upper unit that underwent more intense alteration display greater K enrichment and slightly higher $\delta^{41}K$ values than those from the lower unit (Fig. 1). A composite of interflow sediments (SED) accumulated between basaltic pillows in the upper 230 m of the basement has a $\delta^{41}K$ value of −0.42‰, similar to fresh mid-ocean ridge basalts (MORBs). A grand composite (SUPER) representative of the entire basaltic column has a $\delta^{41}K$ value of −0.32‰ (2SD), which is ~0.1‰ higher than the average $\delta^{41}K$ value of fresh MORBs.

Santiago Ramos *et al.* (*34*) recently reported $\delta^{41}K$ values for 17 samples from the same drill core at depths complementary to this study. Their data have much larger analytical uncertainties and are mostly indistinguishable except for two extreme values (−0.74 and 0.18‰, all their data are converted from seawater scale to reference standard SRM 3141a used in this study) (Fig. 1B). Nevertheless, their samples generally follow the trend defined by our samples, displaying increasing $\delta^{41}K$ upward in the core. Samples adjacent to the hydrothermal layer have substantially higher $\delta^{41}K$ values (Fig. 1B). On the basis of 12 whole-rock samples, Santiago Ramos *et al.* (*34*) calculated an average $\delta^{41}K$ of −0.35 ± 0.18‰ (2SD) weighted by the K/Ti ratios of the samples. Given the large uncertainty with their average, the $\delta^{41}K$ value of the SUPER composite presented here is better constrained (−0.32 ± 0.04‰, 2SD). This composite incorporates various alteration lithologies weighted by their abundance in the core. Hence, the SUPER composite offers a more robust estimate of the bulk composition of altered basaltic basement at ODP Site 801.

Subducting sediments worldwide

Sixty-nine marine sediments recovered from 11 drill sites of the Deep Sea Drilling Project (DSDP) and ODP, along with the sediment composite (SED) from ODP Site 801, were measured to capture the $\delta^{41}K$ variability of sedimentary input to subduction zones on a global scale. Their $\delta^{41}K$ values range from −1.3 to −0.02‰, with the low end reaching nearly 1‰ lighter than the average mantle value of −0.43‰

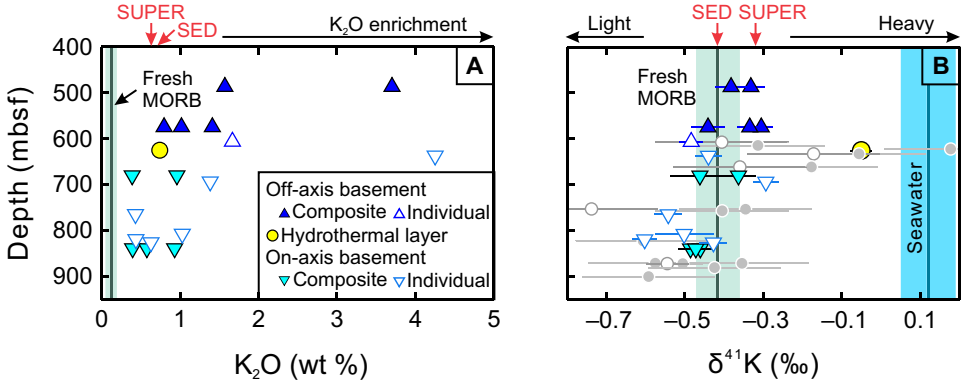

Fig. 1. Potassium content and isotopic composition of altered basaltic basement at ODP Site 801 plotted as a function of depth. (**A**) K_2O, (**B**) $\delta^{41}K$. Depth in mbsf. SUPER refers to the super composite, and SED refers to the interflow sediment composite at Site 801 (*8*). In (A), K_2O contents of altered basalts are from (*8*) and those of fresh MORBs [0.12 ± 0.06 weight % (wt %)] are Site 801 basaltic glass measurements from (*5*). In (B), $\delta^{41}K$ of fresh MORBs is taken from the recommended average for the Japanese basalt standard JB-1 [−0.42 ± 0.06‰ (*27*)]; this basalt is the closest sample to the drill site that has high-precision $\delta^{41}K$ data. Colored symbols are $\delta^{41}K$ data from this study plotted with 95% confidence interval (CI) (table S1). Gray circles are literature data (*34*) from the same drill core but different depths (solid and open symbols represent whole-rock and vein samples, respectively). These data are reported relative to an in-house seawater standard measured at −0.02 ± 0.17‰, and uncertainties are only available as 2SD (*34*). These data are converted to the international K isotopic standard [National Institute of Standards and Technology (NIST) SRM 3141a], to which seawater has a $\delta^{41}K$ value of 0.12 ± 0.07‰ (*30*, *31*).

and the high end approaching the seawater value of 0.12‰ (Fig. 2A). These sediments also display regional variations in $\delta^{41}K$. Detrital sediments (turbidites and terrigenous clays) from Cascadia and Peru have $\delta^{41}K$ values of −0.44 to −0.35‰, similar to the average mantle value. In comparison, those from South Sandwich, Nicobar Fan, Lesser Antilles, and Alaska have $\delta^{41}K$ extending to variably lower values. Notably, most sediments from Lesser Antilles range between −1.0 and −0.7‰. Hydrothermal clays from Ryukyu display even lower $\delta^{41}K$ values down to −1.3‰. On the other hand, four hemipelagic mud sediments from Central America have $\delta^{41}K$ values of −0.37 to −0.27‰, slightly higher than the mantle average. High $\delta^{41}K$ values are also found in oxidized brown clays from the Philippines and Tonga, with an exceptionally high value of −0.02‰ in a Tonga ferromanganese nodule. Overall, the $\delta^{41}K$ variation in these marine sediments is more than double that documented in worldwide loess and shale samples (−0.68 to −0.12‰) from upper continental crust (Fig. 2B) (*23*). Furthermore, greater dispersion in $\delta^{41}K$ occurs in marine sediments with older depositional ages, in particular, toward values lighter than continental $\delta^{41}K$ (Fig. 2B).

DISCUSSION

Our $\delta^{41}K$ data reveal more than 0.5‰ variation in altered oceanic basement from ODP Site 801 and ~1.3‰ variation in marine sediments approaching major subduction zones. The large K isotopic heterogeneity in these crustal components suggests that substantial fractionation occurs during submarine alteration. For detrital sediments, subaerial continental weathering also affected their $\delta^{41}K$ values before they enter the ocean. Below, we examine the direction and extent of associated fractionations and discuss insights that these results provide to the oceanic K cycle and mantle heterogeneity.

Controls of seawater alteration on basaltic crust

Alteration of oceanic crust by low-temperature hydrothermal fluids is associated with substantial enrichments in K (*8*–*10*, *12*, *38*). An earlier study of the Bay of Islands ophiolite, Canada, found that the K added during alteration have seawater-like $\delta^{41}K$ values (*35*), whereas a more comprehensive study on Troodos ophiolite, Cyprus, suggests preferential uptake of light K isotopes by altered basalts (*34*). Given that both ophiolite suites are formed in supra-subduction zone settings where exotic fluids may be discharged from downgoing slabs, they may not be representative of a normal segment of oceanic crust formed at spreading ridges (*12*). For example, Santiago Ramos *et al.* (*34*) argued that K-feldspar dominates the K budget in Troodos ophiolites because its abundance increases positively with K_2O contents in the ophiolite samples. This contrasts with observations from marine basement cores, where K_2O increases coincidingly with H_2O, hence indicating the formation of K-bearing hydrous phases (Fig. 3A) (*12*). This is supported by the observations that the majority of altered basalts from ODP Site 801 have chemical compositions projecting from fresh MORB glass to saponite and celadonite, with a few samples potentially containing a larger amount of Fe oxyhydroxides or zeolites (Fig. 3B). It is thus essential to analyze in situ oceanic basement for comparison with the ophiolites.

The western Pacific basement analyzed here underwent an extensive period of low-temperature hydrothermal alteration, subsequent to a short period of high-temperature hydrothermal alteration at the ridge axis since its formation ~170 Ma ago (*36*). While the K isotopic composition of contemporaneous seawater is unknown, it is suggested that the K^+ concentration in seawater has not changed appreciably during the Phanerozoic (541 Ma to present) (*39*). Furthermore, several late Permian sylvite (KCl) evaporites display $\delta^{41}K$ similar to present-day seawater (*28*, *29*). It is thus reasonable to assume that the $\delta^{41}K$ value of seawater has been more or less constant since the Permian. This assumption is further supported by the indistinguishable average $\delta^{41}K$ values obtained for the ~92-Ma Troodos ophiolites and the ~170-Ma in situ basement at ODP Site 801 [this study and (*34*)].

Our data indicate that altered basalts take up K from seawater with a large K isotope fractionation. At a given $1/[K_2O]$ ratio, the altered basalts have $\delta^{41}K$ values that fall below the binary mixing line between fresh MORB and an infinite seawater reservoir, indicating that secondary minerals formed in basalts preferentially take up light K isotopes from seawater (Fig. 3C). This conclusion holds true even if Jurassic seawater was 0.2‰ lighter than present-day value. The preference for light K by altered basalts is consistent with results from theoretical calculations (*20*) and field studies (*23*–*26*), likely due to weaker K—O bonds in clays than in fluids (*20*). The Si-Fe–rich hydrothermal layer formed between the on- and off-axis basements exhibits the highest $\delta^{41}K$ (−0.05‰) among the sample suite, indicating a dominant seawater influence on the distal hydrothermal fluids (*10*). Samples from the upper unit display a modest decrease in $\delta^{41}K$ with K enrichment, pointing toward a celadonite breccia cement and an interflow sediment sample that is likely rich in celadonite (Fig. 3D). By contrast, samples from the lower unit display a progressive enrichment in heavy K (Fig. 3D). This trend may reflect more restricted access to oxygenated seawater in the lower unit and evolving fluid $\delta^{41}K$, as light K isotopes have been

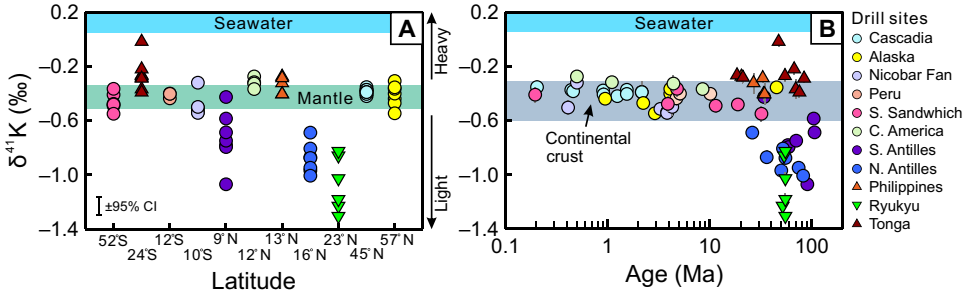

Fig. 2. K isotopic composition of subducting marine sediments. The data reveal (**A**) large regional variation among the 11 drill sites and (**B**) increasing variation with sediment deposition ages. In (A), the horizontal axis (drill site latitude) is not equally spaced to avoid overlap between data from different trenches. Typical $\delta^{41}K$ ranges for the mantle (fig. S1), upper continental crust (*23*), and seawater (*30*, *31*) are plotted for comparison. Sediment $\delta^{41}K$ data are reported in table S2.

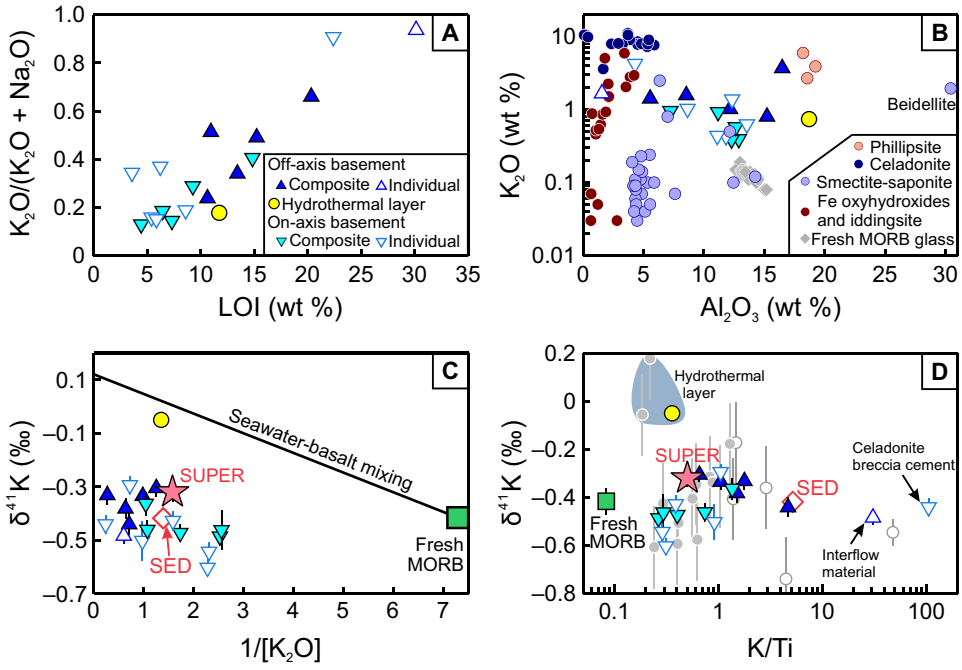

Fig. 3. Variations of K_2O and $\delta^{41}K$ in altered basaltic basement from ODP Site 801. (**A**) and (**B**) indicate that K enrichment is associated with the formation of clay and zeolite minerals. LOI, loss on ignition. In (B), representative secondary minerals reported for Site 801 and the nearby Site 1149 are plotted to identify major K-bearing minerals (*10*, *56*). In (**C**), altered basalts have $\delta^{41}K$ values lower than that expected for binary mixing between an unlimited K reservoir [$\delta^{41}K = 0.12 \pm 0.07$‰ (*30*, *31*)] and fresh MORBs [$K_2O = 0.12$ wt % (*5*), $\delta^{41}K = -0.42 \pm 0.06$‰ (*27*)], suggesting preferential uptake of light K isotopes from seawater during alteration. In (**D**), $\delta^{41}K$ of altered basalts are plotted against the degree of K enrichment assessed by K/Ti ratios. Elemental data for altered basalts are from (*8*), and those for fresh MORBs are Site 801 basaltic glass measurements from (*5*). Gray circles are literature data (*34*) from the same drill core but different depths (solid and open symbols represent whole-rock and vein samples, respectively).

continuously removed into altered basalts. In addition, the slightly higher alteration temperatures at deeper depth may lead to a smaller fractionation between secondary minerals and hydrothermal fluids. Different secondary minerals (e.g., clay versus zeolite; Fig. 3B) can also contribute to $\delta^{41}K$ variability among the altered basalts.

While the K added to altered basalts is significantly lighter than seawater, it does not differ substantially from fresh MORBs. For example, the two celadonite-rich samples have highly enriched K contents, yet their $\delta^{41}K$ values are similar to fresh MORBs (Fig. 3D). Consequently, K enrichment in altered basalts does not produce a substantial shift in $\delta^{41}K$ on bulk-rock scale, with the entire basaltic basement averaging at −0.32‰. These $\delta^{41}K$ features may be typical of altered basement formed at fast-spreading ridges, where oxidation halos along fractures are an order of magnitude less abundant compared to some other altered crustal sections, possibly due to low basement relief and high sedimentation rates (*10*). Exceptionally higher $\delta^{41}K$ values are restricted to samples adjacent to the hydrothermal layers, which is consistent with previous petrographic observations by Alt and Teagle (*10*) that such samples are the most altered. Slow-spreading crust generated in Atlantic and Indian Oceans may acquire higher $\delta^{41}K$ values assisted by fault-enhanced fluid pathways and abundant pillow lavas at depth (*10*, *40*).

Controls of continental weathering and marine diagenesis on sediments

Marine sediments are mixtures of detrital phases, biogenic phases (opal, calcium carbonate, and apatite), and authigenic phases formed in situ in the ocean (*1*, *2*). Biogenic phases have low K contents; nevertheless, they are susceptible to postdepositional dissolution, thereby providing Si and Ca that promote the formation of authigenic minerals. Potassium in marine sediments correlates positively with Rb (Fig. 4A), indicating that both elements are primarily associated with detrital phases, particularly K-feldspar and clay (including mica) that are compatible with the large K cation. The majority of sediments analyzed here share a K_2O/Rb ratio similar to that of Post Archean Australian Shale (PAAS), suggesting that K in these sediments is primarily inherited from subaerial continental weathering. By contrast, many sediments from the Philippines, Tonga, Ryukyu, and Lesser Antilles display elevated K_2O/Rb ratios that are indicative of postdepositional diagenetic K uptake (Fig. 4A), which is consistent with their older depositional ages (Fig. 2B). Except for these sediments, there is a general negative correlation between $\delta^{41}K$ and Rb/K_2O (Fig. 4B). This correlation is reflective of continental weathering, during which the larger Rb cation is preferentially retained over K by clay minerals and heavy K isotopes are preferentially released to the hydrosphere (*23*–*26*). As a result, sediments derived from ancient, highly weathered sources are characterized by higher Rb/K_2O and lower $\delta^{41}K$. In addition to Rb/K_2O, the release of heavy K during continental weathering is further supported by correlations of $\delta^{41}K$ with other weathering indices, such as Cs/K_2O, Rb/Sr, the chemical index of alteration (CIA), and sediment Li contents (fig. S3).

The effect of subaerial continental weathering on the K isotopic compositions of marine sediments is constrained by comparing them with published data on continental sedimentary materials in Fig. 4C. For this comparison, CIA is used as a measure of the weathering of feldspar and volcanic glass to clay minerals (*41*). Terrigenous sediments from Nicobar Fan, Peru, and South Sandwich form a negative correlation between $\delta^{41}K$ values and CIA (Fig. 4C and fig. S3C),

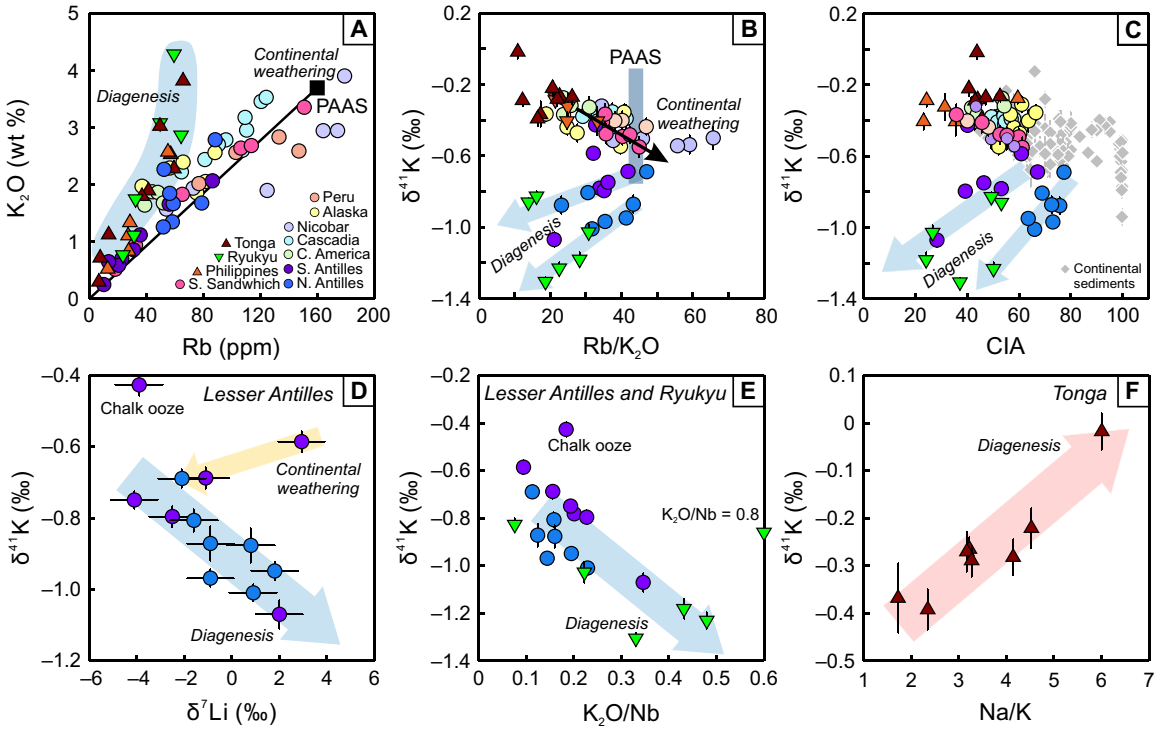

Fig. 4. Major factors controlling K isotope fractionation in marine sediments. (**A**) Positive correlation between K_2O and Rb contents in marine sediments. Sediments with Rb/K_2O ratios similar to PAAS (*57*) are mainly affected by subaerial continental weathering, whereas those with lower Rb/K_2O are possibly subjected to submarine diagenetic K uptake. (**B** and **C**) Preferential release of heavy K isotopes during continental weathering leads to a decrease in $\delta^{41}K$ with increasing weathering in the majority of the samples. $\delta^{41}K$ range for PAAS is from (*23*). In (C), CIA = $100 \times Al_2O_3/(Al_2O_3 + CaO + Na_2O + K_2O)$, where only CaO in the silicates should be considered (*41*). The coupled decrease in $\delta^{41}K$ and CIA in Lesser Antilles and Ryukyu sediments likely reflects diagenetic uptake of K. The gray diamond symbols represent published data on continental sedimentary materials (*23*, *24*, *26*). (**D** and **E**) Preferential uptake of light K isotopes during diagenetic alteration of Ryukyu and Lesser Antilles sediments. (**F**) Diagenetic alteration of Tonga sediments shifts their $\delta^{41}K$ to slightly higher values, possibly due to sorption of heavy K from seawater or pore fluids. Major element data for sediments are from (*52*, *53*).

where the increasing extent of chemical weathering is concomitant with preferential loss of isotopically heavy K. By contrast, no substantial variation in $\delta^{41}K$ is observed for Cascadia and Alaska turbidites (Fig. 4C), suggesting that the increased CIA is mainly caused by weathering of plagioclase rather than K-feldspar, which is more resistant to weathering. This is consistent with their origins from high-latitude regions where physical weathering prevails (Fig. 2A). Moderately to intensively weathered continental sedimentary materials (CIA up to 90) have $\delta^{41}K$ values ranging between −0.70 and −0.35‰ (Fig. 4C). This range is representative of terrigenous sediments delivered to the ocean and is comparable to eolian dust and riverine suspended loads (−0.68 to −0.31‰) (*25*, *26*, *42*). Nonetheless, continental weathering cannot account for the observed broad range in $\delta^{41}K$, and additional processes required are discussed below.

Diagenetic uptake of K in the Ryukyu and Lesser Antilles sediments leads to lowering of Rb/K_2O and CIA that coincides with a decrease in $\delta^{41}K$ to exceptionally low values (Fig. 4, B and C). These correlations indicate that isotopically light K from pore fluids is preferentially incorporated and fixed into authigenic minerals formed in the sediments. This preference is supported by modeling results of sediment pore fluids (*33*), possibly due to a combination of processes occurring during diagenetic K uptake, including a decrease in K—O bond strength (*20*), faster diffusion of ^{39}K to the growing clays (*43*), and preferential loss of ^{41}K during desolvation of hydrated K (*44*). The role of diagenetic alteration is also supported by the negative correlation between $\delta^{41}K$ and $\delta^{7}Li$ for Lesser Antilles sediments (Fig. 4D), which is consistent with the formation of high-$\delta^{7}Li$ diagenetic phases, as opposed to low-$\delta^{7}Li$ clay minerals formed during continental weathering (*45*). In addition, $\delta^{41}K$ values in Ryukyu and Lesser Antilles sediments decrease with increasing K_2O/Nb, suggesting light K enrichment with progressive sediment diagenesis (Fig. 4E).

X-ray diffraction (XRD) analyses on three representative Ryukyu sediments provide additional evidence for preferential uptake of light K by authigenic minerals (fig. S4). Sample 295-3-2-30-35 contains illite-smectite as the only major host of K. Its $\delta^{41}K$ value of −1.2‰ possibly reflects diagenetic transformation of smectite to illite, which may involve dehydration and fixation of K in the interlayer of clays, with both processes favoring light K isotopes as discussed above. Another Ryukyu sediment (294-4-1-110-115) that has a higher $\delta^{41}K$ of −0.86‰ contains a large fraction of illite/smectite (37%) and orthoclase (26%). Its relatively high $\delta^{41}K$ may thus reflect higher $\delta^{41}K$ in K-feldspar relative to clay, which is supported by the measurement of a K-feldspar standard in this study (FK-N; $\delta^{41}K$ = −0.27‰; table S3). The Ryukyu sediment that displays the lowest $\delta^{41}K$ in this study (sample 295-2-6-84-89, −1.3‰) has 27% clinoptilolite (a K-rich zeolite) in addition to 20% illite/smectite, suggesting that clinoptilolite is likely to have exceptionally low $\delta^{41}K$ values. The low $\delta^{41}K$ values in Lesser Antilles sediments are possibly caused by similar diagenetic processes because clinoptilolite is the predominant zeolite in the Atlantic Ocean; furthermore, clinoptilolite is often

associated with calcareous sediments and old sediments (Miocene to Cretaceous) (*46*).

The K-enriched Tonga sediments display $\delta^{41}K$ values slightly higher than terrigenous sediments that underwent little weathering (Fig. 4B) and form a positive correlation with Na/K (Fig. 4F). This correlation is consistent with sorption of isotopically heavy K from high Na/K fluids similar to seawater. Sorption of hydrated K appears to occur with limited isotope fractionation, which is reflected in a ferromanganese nodule that has a $\delta^{41}K$ value close to seawater. Tonga sediments contain abundant bentonite clays that could have strong sorption capabilities (fig. S4). The positive correlation may alternatively suggest formation of authigenic minerals with high Na/K ratios such as phillipsite and merlinoite zeolite. These zeolites can form from abundant amorphous phases in Tonga sediments (fig. S4). Last, K-feldspar and muscovite in Tonga sediments (fig. S4) may also contribute to their slightly higher $\delta^{41}K$ values. Similar diagenetic effects are observed in the Philippines and Central American sediments but are less apparent because of dilution by detrital clays (fig. S3D).

In summary, diagenetic influences are more prominent in sediments that have lower amounts of detrital components. The diagenetic effects on the K isotopic compositions of marine sediments depend primarily on mineral types formed during alteration and the mechanism of K uptake. While sorption of hydrated K may lead to mild enrichment in heavy K isotopes, incorporation of K into authigenic minerals appears to be strongly favoring light K, and in general, marine sediments are a sink for light K isotopes in the ocean.

Implications for oceanic K cycle

Potassium is the fourth most abundant cation in the ocean with a residence time of approximately 10 Ma (*15*). The K concentration and isotopic composition of seawater are thus expected to be in steady state. However, the oceanic K fluxes associated with its primary inputs and outputs remain poorly constrained. A better estimate of K fluxes can be obtained by solving mass and isotope balance equations simultaneously

$$J_{riv} + J_{hyd} = J_{sed} + J_{AOC} \quad (1)$$

$$\delta_{riv}J_{riv} + \delta_{hyd}J_{hyd} = \delta_{sed}J_{sed} + \delta_{AOC}J_{AOC} = (\delta_{sw} + \Delta_{sed})J_{sed} + (\delta_{sw} + \Delta_{AOC})J_{AOC} \quad (2)$$

where the subscripts riv, hyd, sed, and AOC represent the fluxes (J; Tg/year) and $\delta^{41}K$ values (δ; ‰) of K inputs from riverine dissolved loads (riv) and hydrothermal fluids from mid-ocean ridge (hyd), as well as K outputs to marine sediments (sed) and altered oceanic crust (AOC). "Δ" represents K isotope fractionation factors associated with the sediment and AOC sinks. Li *et al.* (*25*) used a Monte Carlo approach to constrain the oceanic K fluxes. Following their approach, we provide a simulation using up-to-date fractionation factors for principle K sources and sinks. This updated model based on our new data incorporates AOC as a sink for light K isotopes in the ocean, as opposed to a fractionation factor of zero used by Li *et al.* (*25*).

Surface runoff is the primary K input to the ocean, delivering 50 to 62 Tg of dissolved K each year (*12*, *13*, *15*). Li *et al.* (*25*) proposed an average $\delta^{41}K$ of −0.22 ± 0.04‰ for global rivers based on a negative correlation of $\delta^{41}K$ in riverine dissolved load with the weathering intensity from 15 river water samples collected in China. A subordinate fraction of K is added to the ocean by mid-ocean ridge hydrothermal fluids, and the estimated flux varies from 5 to 36 Tg (*9*, *11*–*14*). A recent study of high-temperature hydrothermal fluids collected from Gorda Ridge and East Pacific Rise found that these fluids preferentially leach light K isotopes from MORBs, with a fractionation factor of −0.6 to −0.2‰ between fluids and basalts (*32*). Therefore, presently known inputs of K are isotopically lighter than seawater.

Our study indicates that both marine sediments and AOC prefer to take up light K isotopes from seawater. However, the K fluxes associated with these two K sinks are poorly constrained in previous studies, with estimated fluxes varying from 25 to 43.2 Tg/year for marine sediments (*11*–*13*) and from 10 to 19.2 Tg/year for AOC (*12*–*14*, *16*). Here, we use K isotopes to further constrain the K fluxes in the ocean. The K budget in marine sediment reflects a mixture from detrital phases and seawater K incorporated into authigenic minerals. The $\delta^{41}K$ values of −1.3 to −0.22‰ measured in marine sediments suggest a possible range of −1.4 to −0.34‰ for fractionation factors between authigenic minerals and seawater, except for the ferromanganese nodule. The fractionation factor during low-temperature alteration of oceanic crust can be constrained from the SUPER composite that is representative of the entire altered basement drilled at ODP Site 801. The SUPER composite has a K_2O content of 0.62 weight % (wt %) (*8*) and a $\delta^{41}K$ value of −0.32‰. Considering it as a mixture of fresh basalts [K_2O = 0.12 wt % (*5*) and $\delta^{41}K$ = −0.42‰ (*27*)] and an completely altered endmember, the $\delta^{41}K$ of the latter is calculated to be −0.29‰ based on mass balance. Hence, the fractionation factor between altered basalts and seawater is −0.41‰. This value represents a more robust estimate than the slightly lower value of −0.5‰ proposed by Santiago Ramos *et al.* (*34*) based on whole-rock samples from the Site 801 drill core and the Troodos ophiolites; because their average $\delta^{41}K$ value is associated with a large uncertainty of 0.2‰ and does not consider relative contributions from different alteration lithologies.

The ranges of K fluxes and K isotope fractionation factors that solve the mass and isotopic balance are plotted in Fig. 5. The identification of AOC as a light K sink reduces the sediment fluxes from 41 to 52 Tg/year estimated earlier by Li *et al.* (*25*) to between 36 and 43.2 Tg/year. The flux associated with AOC is constrained to vary between 12.4 and 19.2 Tg/year; thus, it can be as high as half of the sediment fluxes. The average fractionation factor during sediment diagenesis is constrained to vary between −0.50 and −0.35‰, which is similar to the fractionation factor of −0.41‰ during low-temperature hydrothermal alteration of the basaltic crust. These similar fractionation factors indicate that the two K sinks are equally efficient in elevating the $\delta^{41}K$ value of seawater, and thus, the $\delta^{41}K$ signature of seawater is insensitive to changes in J_{AOC}/J_{sed}. On the other hand, K leached by hydrothermal fluids circulating at mid-ocean ridges is isotopically lighter than MORBs, whereas riverine waters preferentially leach away heavy K isotopes from continental rocks. As a result, seawater $\delta^{41}K$ will increase in response to an increase in J_{riv}/J_{hyd}. In addition, the $\delta^{41}K$ of riverine input is suggested to be strongly dependent on weathering intensity (*25*). These observations collectively imply a link between continental weathering and marine $\delta^{41}K$ records in sedimentary evaporates, making K isotopes a potential proxy for paleoclimate.

Implications for crustal recycling and mantle heterogeneity

The revealed large variability of $\delta^{41}K$ in subducting oceanic plates has implications for tracing crustal recycling with K isotopes (Fig. 6A).

Although sediment columns investigated here yield a flux-weighted average (−0.48‰; table S5) that is indistinguishable from the mantle, there is a distinguishable inter-arc variation in $\delta^{41}K$ (Fig. 6A). Therefore, sedimentary columns that have more extreme $\delta^{41}K$ may produce a measurable change in the K isotopic composition of local mantle domains. For example, sediments from the Lesser Antilles and Ryukyu arcs are significantly lighter than the mantle, while those from the Philippines and Tonga are slightly heavier (Fig. 6A). It is currently unknown whether K isotopes fractionate during sediment subduction. Yet, studies on exhumed metasediments suggest that subducted sediments retain their K to the depth of arc magma formation (*47*). Therefore, shallow dehydration reactions are expected to have little effect on the K isotopic compositions of the subducting sediments, and melting of sediments is generally required to liberate appreciable amount of K (*48*). The sediment melts will inherit the $\delta^{41}K$ signatures of their precursors because partial melting does not fractionate K isotopes (*19*, *20*). Altered seafloor basalts have $\delta^{41}K$ close to fresh basalts [this study and (*34*)] or substantially higher [−0.17 to 0.19‰ (*21*, *35*)]. On the basis of eclogite studies, dehydration of the basaltic crust is expected to release most of its K to fluids (*49*), with the fluids enriching in heavy K isotopes relative to dehydrated eclogites by a fractionation factor of 1.5‰ (*50*). Therefore, regardless of the $\delta^{41}K$ of basaltic protolith entering subduction zones, dehydration fluids will be considerably heavier than the ambient mantle. The dehydrated crust may then form a low $\delta^{41}K$ (down to −1.6‰) domain in the deep mantle, with much reduced K_2O (<0.3 wt %) (*50*). Overall, the $\delta^{41}K$ imprints of subducted assemblages to the mantle depend apparently on the low-temperature weathering histories of the slabs, the dehydration processes, and the transfer mechanism of K.

A binary mixing calculation is presented to evaluate the sensitivity of mantle $\delta^{41}K$ in response to crustal addition (Fig. 6B). Assuming a global average K concentration for subducting sediments [2.21 wt % (*2*)], an addition of 1 to 3% of Ryukyu or Lesser Antilles sediments to the mantle would produce a sizeable negative shift in $\delta^{41}K$. By contrast, it seems difficult to generate magmas with $\delta^{41}K$ notably higher than the mantle via sediment melt additions. Therefore, low $\delta^{41}K$ in basalts is a sensitive indicator of sediment input (Fig. 6B). Dehydration fluids from altered basalts appear to be a more effective source of heavy K to the mantle than sediment melts. To evaluate their influence, we conservatively use the lowest value of 0.65‰ suggested by Liu *et al.* (*50*) as the high end of $\delta^{41}K$ in dehydration fluids. The low end of $\delta^{41}K$ is taken from the highest AOC value measured in this study (−0.05‰). The average K contents of altered basement from ODP Site 801 (*8*) are taken as an approximation of the K content in dehydration fluids released from the basaltic crust. Under these assumptions, an addition of 3% of such fluids would lead to a notable elevation of $\delta^{41}K$ in the mantle above the slab (Fig. 6B), forming a high-$\delta^{41}K$ reservoir that could contribute to arc magmas or remix into the upper mantle, whereas the dehydrated residual slabs will transfer light K to the deep mantle. The light K may contribute to mantle-derived magmas upon melting, which is readily distinguishable from subducted sediments using radiogenic isotopes. The calculation presented in Fig. 6B suggests that a small

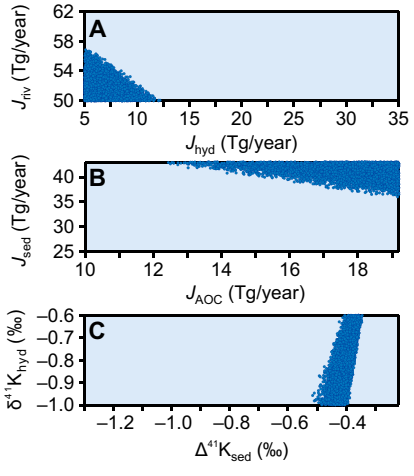

Fig. 5. Oceanic K cycle constrained by K isotopes. Fluxes of K (**A**) into and (**B**) out of the oceans, as well as (**C**) K isotope fractionation factor associated with the sediment sink. The light blue regions represent ranges of J_{hyd}, J_{riv}, J_{AOC}, J_{sed}, and $\delta^{41}K_{hyd}$ reported in the literature (*9*, *11*–*15*, *32*) and $\Delta^{41}K_{sed}$ constrained from sediment $\delta^{41}K$ data reported in this study. The dark blue circles represent solutions from a Monte Carlo simulation that is simultaneously solved for oceanic K mass and isotopic balance.

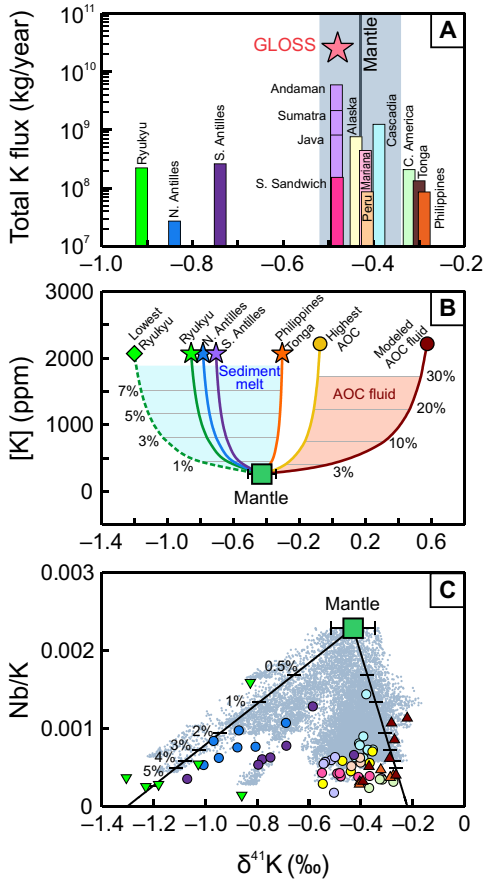

Fig. 6. Sensitivity of $\delta^{41}K$ in tracing recycled crustal materials. (**A**) inter-arc variations in the bulk average of $\delta^{41}K$ for sediment columns investigated here along with their total K flux (see table S5 for details), and (**B**) binary mixing between mantle and sediment melt versus AOC-derived fluids (see the main text for modeling details), and (**C**) random mixing between the mantle and subducted sediments. In (A), the red star denotes flux-weighted average $\delta^{41}K$ of global subducting sediments (GLOSS) based on samples measured in this study. In (C), the small gray dots in the background represent random mixing results from a Monte Carlo simulation. The legends are the same as in Figs. 2 and 4.

contribution from subducted crustal components can cause noticeable $\delta^{41}K$ perturbation on a local mantle domain.

There are currently limited high-precision basalt $\delta^{41}K$ data to evaluate the influence of subducted components in generating mantle heterogeneity. We thus perform a random mixing model between the mantle [260 ppm K and 0.595 ppm Nb (*7*); $\delta^{41}K = -0.43 \pm 0.09$‰ (fig. S1)] and subducting sediments. The Nb/K ratio is used as an indicator of slab input, where K is released to the mantle and Nb is retained in the slab. Modeled results predict a wide variation in $\delta^{41}K$ that extends to considerably low $\delta^{41}K$ values of −1.2‰. This broad range of predicted $\delta^{41}K$ is consistent with recent findings of heterogeneous $\delta^{41}K$ values in mantle peridotites (*51*). The mixing calculation also lends support to previous conclusion that lithospheric mantle modified by subducted sediments is responsible for the formation of low-$\delta^{41}K$ (−0.81 to −0.43‰) potassic basalts from northeastern China (*22*). The modeled results concentrate between −0.6 and −0.2‰, which is comparable to the range of −0.66 to −0.25‰ reported for global oceanic basalts (*19*, *21*), and suggest that recycled sediments may have been involved in the generation of a few oceanic basalts that have $\delta^{41}K$ values deviated from the typical mantle range (fig. S1).

The subduction recycling of crustal K may play an important role in other aspects of the evolution of the mantle given that radiogenic decay of ^{40}K dominates the production of ^{40}Ar and is one of the major heat sources in Earth's interior. The subduction flux of K from global sediments is calculated to be 2.48×10^{10} kg/year based on parameters provided in (*2*), and that from the oceanic crust is 3×10^{10} kg/year (*12*). Together with the large variations of $\delta^{41}K$ observed in some oceanic and continental basalts, recycled K may be pervasively distributed in the mantle, affecting mantle's heat production that powers mantle convection and crustal cycling. Subducted K is also an integral component to be considered in constraining the size of undegassed primitive mantle based on global Ar budget. While ^{40}Ar is lost from the mantle to the atmosphere during volcanic eruption, a substantial portion of K buried in the basaltic crust and sediments is returned to the mantle. Future studies on the K isotopic heterogeneity sampled by arc lavas and oceanic basalts will lead to a better understanding of the fluxes and distribution of various recycled crustal materials in the mantle.

MATERIALS AND METHODS

Samples

Altered oceanic crust

Samples of altered oceanic crust were recovered seaward of the Mariana Trench, from ODP Site 801 that drilled into the oldest basement in the western Pacific (fig. S2). It is a reference basement for consecutive alteration occurring in fast-spreading oceanic crust surrounding the Pacific Ocean and has been well characterized for lithological and geochemical compositions (*8*, *37*, *38*). The basaltic basement comprises a 315-m lower unit formed at the mid-ocean ridge (on-axis; 167.4 Ma) and a 175-m upper unit formed approximately 400 to 600 km away from the spreading ridges (off-axis; 160.1 Ma) (*36*). The basement contains eight lithological units (*38*), including ~60 m of transitional/alkali basalts and ~400 m of three tholeiitic MORB units that differ in relative abundance of massive/sheet flow, pillows, and intercalated sediments. In addition to a 10-m breccia layer, two Si-Fe–rich hydrothermal layers are observed in the core, which are not commonly seen in other drilled basement (*10*).

The alteration history recorded in the core has been studied by Alt and Teagle (*10*) in detail. Secondary minerals observed in the basement are characteristic of low-temperature alteration (<100°C), including the formation of celadonite and Fe oxyhydroxides in relatively oxidized fluids, followed by saponite and pyrite formation in more reduced fluids, and finally calcite precipitation. The alteration temperatures constrained from oxygen isotopes in phyllosilicate and calcite generally increase downward. The upper unit typically underwent higher degree of alteration than the lower unit (30 to 80% versus 10 to 20%), probably related to more pervasive and longer duration of seawater circulation in the upper unit, assisted by a denser network of open veins. In contrast, fluid pathways in the lower unit are sealed by secondary mineral precipitation during the preceding low-temperature hydrothermal circulation that forms the silica-iron deposit.

Subducting sediments

Sediment samples (fig. S2) were selected to cover a wide range of sedimentary lithologies, fluxes, and compositions; they were used for establishing the chemical and isotopic characteristics of the global subducting sediments (*1*, *2*, *52*–*54*). Among them, sedimentary columns that are near continental margins, including the Cascadia, Alaska, and Antilles, are dominated by thick turbiditic sequences. In addition, Himalayan-derived turbidites comprise a large portion of the Java-Sumatra column. Further away from land, sedimentary columns from South Sandwich, Central American, and Peru trenches comprise pelagic/hemipelagic clay mixed with volcanic ash and siliceous oozes and sometimes overlying a carbonate layer. By contrast, sediments approaching the Philippines, Tonga, and Ryukyu trenches are featured by slowly deposited metalliferous brown to black clays with a prominent input from hydrogenous and hydrothermal components. These sediments contain much higher concentrations of FeO (>25 wt %), MnO (~2 wt %), Ba, and Pb than sediments derived from continental weathering.

Methods

Potassium isotope analysis

Potassium extraction and isotopic measurement were performed at the Isotope Laboratory of the University of Washington, Seattle. Approximately 10- to 30-mg sample powders were dissolved in screw-top Teflon beakers with an acid mixture of Optima-grade HF-HNO_3-HCl. A few drops of Optima-grade H_2O_2 were added to organic-rich samples. Potassium was purified using cation exchange chromatography (2 ml; Bio-Rad AG50W-X8, 200 to 400 mesh) with double-distilled 0.5 N HNO_3 as the eluent (*27*). The separation was repeated to ensure the high purity of the K fractions. At least one standard was processed along with samples for each batch of column chemistry. The procedural blank is less than 10 ng, which is negligible compared to the amount of K (100 to 200 μg) loaded onto the columns.

Potassium isotopic ratios were measured on a Nu Plasma II multicollector inductively coupled plasma mass spectrometer in high–mass resolution mode operating at reduced Radio frenquency (RF) power with a DSN-100 desolvation nebulizer system to suppress the formation of argon-based interferences, particularly $^{40}Ar^{1}H^{+}$ (*18*). $^{41}K^{+}$ and $^{39}K^{+}$ were measured simultaneously on interference-free peak shoulders with the subtraction of on-peak zero values. On-peak zero on mass 41 typically varies between -8×10^{-4} and -1.5×10^{-3} V and that on mass 39 is around -3×10^{-3} V; these backgrounds are negligible compared to the signals of sample solutions (typically 4

to 10 V). Instrumental mass bias was corrected by bracketing sample measurement with measurements on a K standard (SRM 3141a) from the National Institute of Standards and Technology (NIST). Potassium isotopic data are reported relative to this standard in δ notation, following the recommendation by Hu *et al.* (*18*)

$$\delta^{41}\mathrm{K}\,(‰) = \left\{ \frac{(^{41}\mathrm{K}/^{39}\mathrm{K})_{\mathrm{sample}}}{(^{41}\mathrm{K}/^{39}\mathrm{K})_{\mathrm{NIST\ SRM\ 3141a}}} - 1 \right\} \times 1000$$

At least one standard was analyzed during each session as an unknown to evaluate accuracy and reproducibility (table S3). Standards of basalt (BHVO-1), granite (G-2), and mica schist (SDC-1) yield similar δ^{41}K values from −0.47 to −0.41‰, whereas the shale standard (SGR-1) has a significantly higher δ^{41}K value of −0.24‰. A similar δ^{41}K value of −0.27‰ has been measured in a potash feldspar standard (FK-N). The Hawaiian seawater standard has the highest δ^{41}K value of 0.14‰. All these values agree with published data (*18*, *27*, *30*, *31*, *55*). In addition, δ^{41}K values for duplicates (repeat instrumental measurement) and replicates (repeat dissolution and column chemistry) are reproducible within ±0.06‰ at 95% confidence interval (CI).

XRD analysis

Mineralogy was determined in five representative sediment samples from DSDP Sites 294/295 and Site 596. They were analyzed using a Rigaku MiniFlex 600 benchtop x-ray diffractometer (XRD) fitted with a D/teX high-speed detector and Co Kα radiation at the NASA Johnson Space Center. Diffraction data were collected at a step size of 0.02° per minute step counting rate, from 2 to 80° 2θ at 15 mA and 40 kV. Samples were mounted in aluminum holders, and the instrument was operated under ambient conditions and calibrated with a NIST silicon standard. A NIST lanthanum hexaboride standard is used to characterize the instrument line broadening function. Rietveld refinement is carried out using MDI Jade Software with initial structure parameters for crystalline phases from the RRUFF database. Background patterns were fit by a polynomial, and peaks were modeled by a pseudo-Voigt profile function. Pattern overlays of standard phyllosilicates (Clay Mineral Repository) with known reference intensity ratio (RIR) and full width at half maximum (FWHM) were used in Rietveld refinements to estimate abundances of phyllosilicates in bulk samples.

SUPPLEMENTARY MATERIALS

Supplementary material for this article is available at http://advances.sciencemag.org/cgi/content/full/6/49/eabb2472/DC1

REFERENCES AND NOTES

1. T. Plank, C. H. Langmuir, The chemical composition of subducting sediment and its consequences for the crust and mantle. *Chem. Geol.* **145**, 325–394 (1998).
2. T. Plank, The chemical composition of subducting sediments, in *Treatise on Geochemistry*, H. D. Holland, K. K. Turekian, Eds. (Elsevier, ed. 2, 2014), pp. 607–629.
3. J. G. Ryan, C. Chauvel, The subduction-zone filter and the impact of recycled materials on the evolution of the mantle, in *Treatise on Geochemistry* H. D. Holland, K. K. Turekian, Eds. (Elsevier, ed. 2, 2014), pp. 479–508.
4. M. G. Jackson, R. Dasgupta, Compositions of HIMU, EM1, and EM2 from global trends between radiogenic isotopes and major elements in oceanic island basalts. *Earth Planet. Sci. Lett.* **276**, 175–186 (2008).
5. M. Fisk, K. A. Kelley, Probing the Pacific's oldest MORB glass: Mantle chemistry and melting conditions during the birth of the Pacific Plate. *Earth Planet. Sci. Lett.* **202**, 741–752 (2002).
6. W. M. White, E. M. Klein, in *Treatise on Geochemistry*, H. D. Holland, K. K. Turekian, Eds. (Elsevier, ed. 2, 2014), pp. 457–496.
7. H. Palme, H. S. C. O'Neill, Cosmochemical estimates of mantle composition, in *Treatise on Geochemistry*, H. D. Holland, K. K. Turekian, Eds. (Elsevier, ed. 2, 2014), pp. 1–39.
8. K. A. Kelley, T. Plank, J. Ludden, H. Staudigel, Composition of altered oceanic crust at ODP Sites 801 and 1149. *Geochem. Geophys. Geosys.* **4**, 8910 (2003).
9. H. Staudigel, Chemical fluxes from hydrothermal alteration of the oceanic crust, in *Treatise on Geochemistry*, H. D. Holland, K. K. Turekian, Eds. (Elsevier, ed. 2, 2014), pp. 583–606.
10. J. C. Alt, D. A. H. Teagle, Hydrothermal alteration of upper oceanic crust formed at a fast-spreading ridge: Mineral, chemical, and isotopic evidence from ODP Site 801. *Chem. Geol.* **201**, 191–211 (2003).
11. S. Bloch, J. L. Bischoff, The effect of low-temperature alteration of basalt on the oceanic budget of potassium. *Geology* **7**, 193–196 (1979).
12. R. D. Jarrard, Subduction fluxes of water, carbon dioxide, chlorine, and potassium. *Geochem. Geophys. Geosys.* **4**, 8905 (2003).
13. H. D. Holland, Sea level, sediments and the composition of seawater. *Am. J. Sci.* **305**, 220–239 (2005).
14. H. Elderfield, A. Schultz, Mid-ocean ridge hydrothermal fluxes and the chemical composition of the ocean. *Annu. Rev. Earth Planet. Sci.* **24**, 191–224 (1996).
15. E. K. Berner, R. A. Berner, *Global Environment: Water, Air, and Geochemical Cycles* (Princeton Univ. Press, 2012).
16. A. J. Spivack, H. Staudigel, Low-temperature alteration of the upper oceanic crust and the alkalinity budget of seawater. *Chem. Geol.* **115**, 239–247 (1994).
17. M. Humayun, R. N. Clayton, Precise determination of the isotopic composition of potassium: Application to terristrial rocks and lunar soils. *Geochim. Cosmochim. Acta* **59**, 2115–2130 (1995).
18. Y. Hu, X.-Y. Chen, Y.-K. Xu, F.-Z. Teng, High-precision analysis of potassium isotopes by HR-MC-ICPMS. *Chem. Geol.* **493**, 100–108 (2018).
19. B. Tuller-Ross, P. S. Savage, H. Chen, K. Wang, Potassium isotope fractionation during magmatic differentiation of basalt to rhyolite. *Chem. Geol.* **525**, 37–45 (2019).
20. H. Zeng, V. F. Rozsa, N. X. Nie, Z. Zhang, T. A. Pham, G. Galli, N. Dauphas, Ab initio calculation of equilibrium isotopic fractionations of potassium and rubidium in minerals and water. *ACS Earth Space Chem.* **3**, 2601–2612 (2019).
21. B. Tuller-Ross, B. Marty, H. Chen, K. A. Kelley, H. Lee, K. Wang, Potassium isotope systematics of oceanic basalts. *Geochim. Cosmochim. Acta* **259**, 144–154 (2019).
22. Y. Sun, F.-Z. Teng, Y. Hu, X.-Y. Chen, K.-N. Pang, Tracing subducted oceanic slabs in the mantle by using potassium isotopes. *Geochim. Cosmochim. Acta* **278**, 353–360 (2020).
23. T.-Y. Huang, F.-Z. Teng, R. L. Rudnick, X.-Y. Chen, Y. Hu, Y.-S. Liu, F.-Y. Wu, Heterogeneous potassium isotopic composition of the upper continental crust. *Geochim. Cosmochim. Acta* **278**, 122–136 (2020).
24. F.-Z. Teng, Y. Hu, J. Ma, G. Wei, Potassium isotope fractionation during continental weathering and implications for global K isotopic balance. *Geochim. Cosmochim. Acta* **278**, 261–271 (2020).
25. S. Li, W. Li, B. L. Beard, M. E. Raymo, X. Wang, Y. Chen, J. Chen, K isotopes as a tracer for continental weathering and geological K cycling. *Proc. Natl. Acad. Sci. U.S.A.* **116**, 8740–8745 (2019).
26. H. Chen, X.-M. Liu, K. Wang, Potassium isotope fractionation during chemical weathering of basalts. *Earth Planet. Sci. Lett.* **539**, 116192 (2020).
27. Y.-K. Xu, Y. Hu, X.-Y. Chen, T.-Y. Huang, R. S. Sletten, D. Zhu, F.-Z. Teng, Potassium isotopic compositions of international geological reference materials. *Chem. Geol.* **513**, 101–107 (2019).
28. K. Wang, S. B. Jacobsen, An estimate of the Bulk Silicate Earth potassium isotopic composition based on MC-ICPMS measurements of basalts. *Geochim. Cosmochim. Acta* **178**, 223–232 (2016).
29. L. E. Morgan, D. P. Santiago Ramos, B. Davidheiser-Kroll, J. Faithfull, N. S. Lloyd, R. M. Ellam, J. A. Higgins, High-precision ^{41}K/^{39}K measurements by MC-ICP-MS indicate terrestrial variability of δ^{41}K. *J. Anal. Atom. Spectrom.* **33**, 175–186 (2018).
30. K. Wang, H. G. Close, B. Tuller-Ross, H. Chen, Global average potassium isotope composition of modern seawater. *ACS Earth Space Chem.* **4**, 1010–1017 (2020).
31. M. Hille, Y. Hu, T.-Y. Huang, F.-Z. Teng, Homogeneous and heavy potassium isotopic composition of global oceans. *Sci. Bull.* **64**, 1740–1742 (2019).
32. X. Y. Zheng, B. L. Beard, M. Neuman, M. F. Fahnestock, J. G. Bryce, C. Johnson, Constraining stable K isotope mass balance of the global ocean and its implications for the modern and past silicate cycle [abstract EP33C-2361]. *Am. Geophys. Union Fall Meet.* (2019).
33. D. P. Santiago Ramos, L. E. Morgan, N. S. Lloyd, J. A. Higgins, Reverse weathering in marine sediments and the geochemical cycle of potassium in seawater: Insights from the K isotopic composition (^{41}K/^{39}K) of deep-sea pore-fluids. *Geochim. Cosmochim. Acta* **236**, 99–120 (2018).
34. D. P. Santiago Ramos, L. A. Coogan, J. G. Murphy, J. A. Higgins, Low-temperature oceanic crust alteration and the isotopic budgets of potassium and magnesium in seawater. *Earth Planet. Sci. Lett.* **541**, 116290 (2020).
35. C. A. Parendo, S. B. Jacobsen, K. Wang, K isotopes as a tracer of seafloor hydrothermal alteration. *Proc. Natl. Acad. Sci. U.S.A.* **114**, 1827–1831 (2017).

36. A. A. P. Koppers, H. Staudigel, R. A. Duncan, High-resolution $^{40}Ar/^{39}Ar$ dating of the oldest oceanic basement basalts in the western Pacific basin. *Geochem. Geophys. Geosys.* **4**, 8914 (2003).
37. J. N. Ludden, T. Plank, R. Larson, C. Escutia, Leg 185 Synthesis: Sampling the oldest crust in the ocean basins to understand Earth's geodynamic and geochemical fluxes. *Proc. Ocean Drill. Prog. Sci. Res.* **185**, 1–35 (2006).
38. T. Plank, J. N. Ludden, C. Escutia, Leg 185 summary: Inputs to the Izu-Mariana subduction system. *Proc. Ocean Drill. Prog. Init. Res.* **185**, 1–63 (2000).
39. J. Horita, H. Zimmermann, H. D. Holland, Chemical evolution of seawater during the Phanerozoic: Implications from the record of marine evaporites. *Geochim. Cosmochim. Acta* **66**, 3733–3756 (2002).
40. R. Gao, J. C. Lassiter, J. D. Barnes, D. A. Clague, W. A. Bohrson, Geochemical investigation of gabbroic xenoliths from Hualalai volcano: Implications for lower oceanic crust accretion and Hualalai Volcano magma storage system. *Earth Planet. Sci. Lett.* **442**, 162–172 (2016).
41. H. W. Nesbitt, G. M. Young, Early Proterozoic climates and plate motions inferred from major element chemistry of lutites. *Nature* **299**, 715–717 (1982).
42. X. Li, G. Han, Q. Zhang, Z. Miao, An optimal separation method for high-precision K isotope analysis by using MC-ICP-MS with a dummy bucket. *J. Anal. Atom. Spectrom.* **35**, 1330–1339 (2020).
43. I. C. Bourg, F. M. Richter, J. N. Christensen, G. Sposito, Isotopic mass dependence of metal cation diffusion coefficients in liquid water. *Geochim. Cosmochim. Acta* **74**, 2249–2256 (2010).
44. A. E. Hofmann, I. C. Bourg, D. J. DePaolo, Ion desolvation as a mechanism for kinetic isotope fractionation in aqueous systems. *Proc. Natl. Acad. Sci. U.S.A.* **109**, 18689–18694 (2012).
45. M. Tang, R. L. Rudnick, C. Chauvel, Sedimentary input to the source of Lesser Antilles lavas: A Li perspective. *Geochim. Cosmochim. Acta* **144**, 43–58 (2014).
46. S. A. Stonecipher, Origin, distribution and diagenesis of phillipsite and clinoptilolite in deep-sea sediments. *Chem. Geol.* **17**, 307–318 (1976).
47. V. Busigny, P. Cartigny, P. Philippot, M. Ader, M. Javoy, Massive recycling of nitrogen and other fluid-mobile elements (K, Rb, Cs, H) in a cold slab environment: Evidence from HP to UHP oceanic metasediments of the Schistes Lustrés nappe (western Alps, Europe). *Earth Planet. Sci. Lett.* **215**, 27–42 (2003).
48. M. C. Johnson, T. Plank, Dehydration and melting experiments constrain the fate of subducted sediments. *Geochem. Geophys. Geosys.* **1**, 1007 (2000).
49. H. Becker, K. P. Jochum, R. W. Carlson, Trace element fractionation during dehydration of eclogites from high-pressure terranes and the implications for element fluxes in subduction zones. *Chem. Geol.* **163**, 65–99 (2000).
50. H. Liu, K. Wang, W.-D. Sun, Y. Xiao, Y.-Y. Xue, B. Tuller-Ross, Extremely light K in subducted low-T altered oceanic crust: Implications for K recycling in subduction zone. *Geochim. Cosmochim. Acta* **277**, 206–223 (2020).
51. D. A. Ionov, K. Wang, Potassium isotope composition of mantle peridotite, abstract presented at the Goldschmidt Conference, Honolulu (2020); https://doi.org/10.46427/gold2020.1142.
52. J. D. Vervoort, T. Plank, J. Prytulak, The Hf–Nd isotopic composition of marine sediments. *Geochim. Cosmochim. Acta* **75**, 5903–5926 (2011).
53. M. Carpentier, C. Chauvel, N. Mattielli, Pb–Nd isotopic constraints on sedimentary input into the Lesser Antilles arc system. *Earth Planet. Sci. Lett.* **272**, 199–211 (2008).
54. Y. Hu, F.-Z. Teng, T. Plank, K.-J. Huang, Magnesium isotopic composition of subducting marine sediments. *Chem. Geol.* **466**, 15–31 (2017).
55. H. Chen, Z. Tian, B. Tuller-Ross, R. L. Korotev, K. Wang, High-precision potassium isotopic analysis by MC-ICP-MS: An inter-laboratory comparison and refined K atomic weight. *J. Anal. Atom. Spectrom.* **34**, 160–171 (2019).
56. E. H. Talbi, J. Honnorez, Low-temperature alteration of mesozoic oceanic crust, Ocean Drilling Program Leg 185. *Geochem. Geophys. Geosys.* **4**, 8906 (2003).
57. S. R. Taylor, S. M. McLennan, *The Continental Crust: Its Composition and Evolution* (U.S. Department of Energy, 1985).
58. P. Vermeesch, On the visualisation of detrital age distributions. *Chem. Geol.* **312–313**, 190–194 (2012).

Acknowledgments: We would like to thank M. Jiang and W. Lindsay for assistance in the laboratory and R. Sletten for stimulating discussions and editing. We are grateful to D. Ming and V. Tu for the XRD analysis at the NASA Johnson Space Center and to X. Yang for assistance with modeling. Constructive comments from K. Wang, an anonymous reviewer, and the associate editor are greatly appreciated. **Funding:** F.-Z.T. acknowledges funding from NSF (EAR-17407706). This is IPGP contribution no. 4162. **Author contributions:** Y.H. and F.-Z.T. designed the research. Y.H. conducted the analytical work. T.P. and C.C. provided samples. All authors participated in the interpretation of the data. The manuscript was written by Y.H. and F.-Z.T. with input from T.P. and C.C. **Competing interests:** The authors declare that they have no competing interests. **Data and materials availability:** All data needed to evaluate the conclusions in the paper are present in the paper and/or the Supplementary Materials. Additional data related to this paper may be requested from the authors.

Submitted 11 February 2020
Accepted 19 October 2020
Published 2 December 2020
10.1126/sciadv.abb2472

Citation: Y. Hu, F.-Z. Teng, T. Plank, C. Chauvel, Potassium isotopic heterogeneity in subducting oceanic plates. *Sci. Adv.* **6**, eabb2472 (2020).